Processing of Multiresolution Thermal Hyperspectral and Digital Color Data: Outcome of the 2014 IEEE GRSS Data Fusion Contest

Wenzhi Liao, *Member, IEEE*, Xin Huang, *Senior Member, IEEE*, Frieke Van Coillie, Sidharta Gautama, *Member, IEEE*, Aleksandra Pižurica, *Member, IEEE*, Wilfried Philips, *Senior Member, IEEE*, Hui Liu, Tingting Zhu, Michal Shimoni, *Member, IEEE*, Gabriele Moser, *Senior Member, IEEE*, and Devis Tuia, *Senior Member, IEEE*

***Abstract*—This paper reports the outcomes of the 2014 Data Fusion Contest organized by the Image Analysis and Data Fusion Technical Committee (IADF TC) of the IEEE Geoscience and Remote Sensing Society (IEEE GRSS). As for previous years, the IADF TC organized a data fusion contest aiming at fostering new ideas and solutions for multisource remote sensing studies. In the 2014 edition, participants considered multiresolution and multisensor fusion between optical data acquired at 20-cm resolution and long-wave (thermal) infrared hyperspectral data at 1-m resolution. The Contest was proposed as a double-track competition: one aiming at accurate landcover classification and the other seeking innovation in the fusion of thermal hyperspectral and color data. In this paper, the results obtained by the winners of both tracks are presented and discussed.**

***Index Terms*—Hyperspectral, image analysis and data fusion (IADF), landcover classification, multimodal-, multiresolution-, multisource-data fusion, thermal imaging.**

I. Introduction

REMOTE sensing has overcome the limits of its own discipline. Data acquired by sensors mounted on unmanned, airborne, or satellite platforms are used by many scientific disciplines, in public administrations, and in everyday's life. Due to this tremendous (and far from being over) increase in notoriety, the discipline faces strong pressure for providing methodologies capable of offering a wide variety of products using an even larger set of acquisition technologies, each one with its own specific physical and signal properties. Modern remote sensing is a science that must answer this call: providing information of the highest quality with the data that are available [1].

If the problem is certainly not new—people have been carrying research in data fusion for decades [2]—what changed is the amount of data and the diversity of sensors that are available to the community. We are no more confronted with problems related to the lack of data, we are rather overwhelmed by data of each kind and must be capable of making some sense out of it in the light of answering a scientific societal question [3]. In this context, image analysis and data fusion have also evolved and nowadays play several roles, going from the historical precursors, pansharpening [4], [5], classification [6]–[8], and change detection [9], to new areas such as large-scale processing [10], [11], multiple resolutions [12], [13], domain adaptation [14]–[16], interactive systems [17], [18], and integration of signal modalities with various meanings and properties [19].

The Image Analysis and Data Fusion Technical Committee (IADF TC) of the Geoscience and Remote Sensing Society (GRSS) is an international network of scientists active in these fields and, in particular, in multitemporal, multisource, multiresolution, and multimodal remote sensing image analysis. IADF TC serves as a gathering point for scientists, industry professionals, and students interested in image analysis and data fusion. To foster emergence of new ideas and the establishment of best practices, it organizes an annual contest, which is open to the international remote sensing community. Since 2006, the Data Fusion Contest (DFC) has gathered the image analysis community and fostered innovation around challenging topics of multisource remote sensing, including pansharpening [4], radar and optical classification [20]–[22], hyperspectral classification [23], multiangular data [24], and large-scale classification [25].

The 2014 edition of the Contest tackled two of the most open problems of the community: handling data 1) from multiple sources and 2) at multiple resolutions. The aim was to

Manuscript received October 31, 2014; revised February 17, 2015; accepted March 26, 2015. Date of publication May 14, 2015; date of current version July 30, 2015. The work of D. Tuia was supported by the Swiss National Science Foundation (project 150593: "Multimodal machine learning for remote sensing information fusion") and the work of W. Liao, A. Pizurica, S. Gautama, W. Philips, and F. Van Coillie was supported in part by the SBO-IWT (project Chameleon "Domain-specific Hyperspectral Imaging Systems for Relevant Industrial Applications") and in part by the FWO (project G037115N: Data fusion for image analysis in remote sensing).

W. Liao, S. Gautama, A. Pižurica, and W. Philips are with Ghent University-TELIN-IPI-iMinds, Ghent 9000, Belgium (e-mail: wliao@telin.ugent.be).

F. Van Coillie is with the FORSIT Research Unit, Ghent University, Ghent 9000, Belgium (e-mail: Frieke.VanCoillie@ugent.be).

X. Huang, H. Liu, and T. Zhu are with the State Key Laboratory of Information Engineering in Surveying, Mapping, and Remote Sensing, Wuhan University, Wuhan 430079, China (e-mail: huang_whu@163.com).

M. Shimoni is with the Signal and Image Centre, Department of Electrical Engineering, Royal Military Academy (SIC-RMA), Brussels 1000, Belgium (e-mail: mshimoni@elec.rma.ac.be).

G. Moser is with the Department of Electrical, Electronic, Telecommunications Engineering and Naval Architecture (DITEN), University of Genoa, Genoa I-16145, Italy (e-mail: gabriele.moser@unige.it).

D. Tuia is with the Department of Geography, University of Zurich, Zurich 8057, Switzerland (e-mail: devis.tuia@geo.uzh.ch).

Color versions of one or more of the figures in this paper are available online at http://ieeexplore.ieee.org.

Digital Object Identifier 10.1109/JSTARS.2015.2420582

investigate the possible synergies between two types of data, which are becoming more and more popular and that carry complementary information: very-high-resolution data (20-cm resolution) acquired by a digital color camera (three channels in the visible range) and a new data type for a data fusion contest: a 1-m resolution hyperspectral image in the long-wave (thermal) infrared domain.

Thermal infrared is a very challenging data source with high potential: it examines the spectral emitted radiance differences between target objects in the thermal infrared, so it can perform target detection and material classification regardless of illumination conditions. The physical background is the fundamental spectral absorption features of silicate minerals, which are the major components of the terrestrial surface and the primary constituent of man-made construction objects. The silicon–oxygen bonds of these silicate minerals (Si–O) do not produce spectral features in the visible-to-shortwave infrared region of the spectrum ($0.4-2.5\ \mu\mathrm{m}$) [26]. However, the stretching vibrations of the Si-O bonds produce strong fundamental features in the long-wave infrared (LWIR, thermal infrared) spectral wavelengths ($8-12\ \mu\mathrm{m}$), the so-called "Reststrahlen bands" [27]. Man-made objects also tend to emit IR radiation that is polarized to a greater extent than naturally derived background materials (i.e., trees, soil, vegetation) [28]–[30]. This is attributed to the fact that man-made objects tend to have surface features that are relatively smooth compared to most naturally occurring surfaces. If surface irregularities are large compared to the wavelength of the emitted radiation, the total emissivity may suffice as the primary parameter of interest. However, if surface irregularities are small compared to the emission wavelength, the surface tends to be more specular and an observable induced polarization occurs in the emitted thermal radiation [31]. These fundamentals were used for the development of spectral-based methods for urban classification [31], [32] or unmixing of man-made materials [33], [34] using LWIR hyperspectral data.

Despite its attractiveness, fusion in the thermal domain has been studied only scarcely in the IADF community (some exceptions can be found in pansharpening [35], [36] or in the blending of medium (MODIS) and high (Landsat) resolution data [37]), but is attracting increasing interest, e.g., for the fusion of thermal data acquired by unmanned aerial vehicles (UAVs) with airborne hyperspectral images (APEX, for example) [38]–[40] or with digital cameras.

Following the structure proposed in 2013 [22], the DFC 2014 consisted of two parallel tracks of equal importance:

1) *Classification Contest*: This track focused on classification results with the aim of providing a fair comparison of best practices and approaches to the classification with these new types of sensors. The aim was to obtain the most accurate classification map as possible. To assess accuracy, two aspects were considered: the first was the ability to generalize the result to zones wider than the training area. To assess such requirement, the data were delivered in two stages: first, a small, geographically concentrated portion was delivered along with the associated ground truth; later on, the rest of the image, on which the classification accuracy was evaluated by using an undisclosed test set, was also released. The second aspect was the computational complexity. To constrain it, we allowed only a limited time window for providing the final map. Moreover, only a single map could be submitted by each participating team during the 2 weeks following the disclosure of the test data. Ranking was based on the accuracy of the submitted classification map with respect to the aforementioned undisclosed test set. Methodological novelty was not among the evaluation criteria.
   The Classification Contest was won by the team comprised of *X. Huang*, *H. Liu*, and *T. Zhu* from Wuhan University (China).
2) *Paper Contest*: The paper contest was set up as an incubator for new ideas for the processing of multiresolution data and in particular for the analysis of thermal hyperspectral data at such a high resolution, which are a modality quite new for the IADF TC community. For this reason, no topic was imposed by the organizers and the deliverable was a four-page manuscript addressing the problem considered, the methodology adopted, and the results obtained. For this second competition, the temporal deadline was looser and the winners were selected by an Award Committee on the basis of two criteria: the novelty of the problem considered and the technical-scientific interest of the approach proposed. The Paper Contest was awarded to the team composed of *W. Liao*, *F. Van Coillie*, *S. Gautama*, *A. Pizurica*, and *W. Philips* from Ghent University (Belgium).

The two winning teams were awarded during the 2014 IEEE International Geoscience and Remote Sensing Symposium (IGARSS) held in Québec City, Canada. Each winning team received IEEE GRSS Certificates of Appreciation and a Google Nexus 7 tablet, sponsored by the GRSS.

This paper presents the contributions awarded and opens a discussion fostered by the results of the Contest. It aims at assessing the health and future of image analysis and data fusion in remote sensing. It is organized as follows: Section II presents the datasets used in detail, as well as the contest schedule. Section III summarizes and compares the two awarded approaches, which are then presented in Sections IV (classification track) and V (paper track), respectively. In Section VI, the results obtained and the trends observed during the contest are discussed, while some conclusions are drawn in Section VII.

II. Challenge of 2014: Multiresolution Multisensor Data

The 2014 Contest involved two airborne datasets acquired at different spectral ranges and spatial resolutions: 1) a coarser-resolution LWIR hyperspectral image and 2) fine-resolution visible (VIS) imagery (Fig. 1). The data were acquired and were provided for the Contest by Telops Inc., Québec, Canada.[1] They cover an urban area near Thetford Mines in Québec, Canada, including residential and commercial buildings, roads,

[1] [Online]. Available: http://www.telops.com

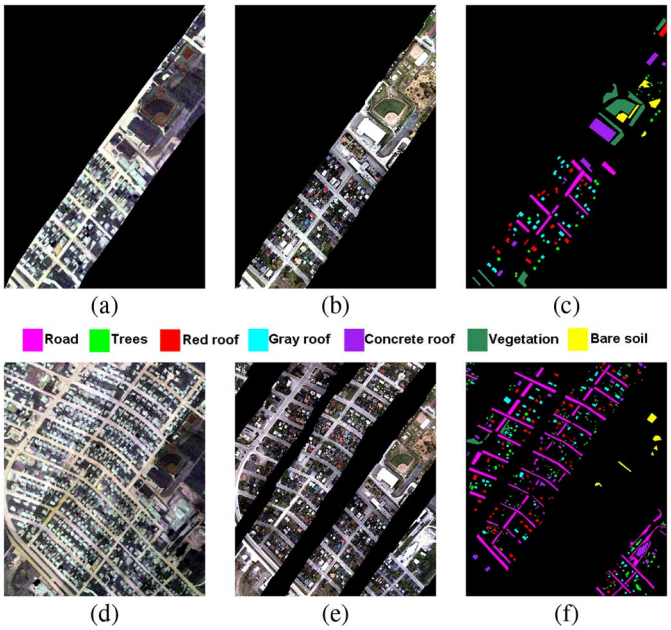

Fig. 1. Data set for the 2014 Data Fusion Contest: top row denotes the subset of the data provided for training in the first stage of the contest: (a) RGB false-color composite of three channels of the LWIR image (1-m resolution); (b) color data (20-cm resolution); (c) training labels. The bottom row illustrates the data released for testing in the second phase: (d) LWIR data; (e) color data. The ground truth in (f) was used by the committee to evaluate the classification maps and was not provided to the participants.

and gardens. The two airborne data were acquired on May 21, 2013 using two different platforms with a short temporal gap. The average height of both LWIR and visible sensors above ground was 2650 ft (807 m), resulting in an average spatial resolution (ground sample distance, GSD) of approximately 1 m for the LWIR imagery and 0.1 m for the VIS imagery. The visible data used for the contest have been sampled to 0.2 m for reducing the resolution ratio between the two data sources.

The LWIR data [Fig. 1(a) and (d)] were acquired using the Telops Hyper-Cam, an airborne long-wave infrared hyperspectral imager [41]. It is a Fourier-transform spectrometer (FTS) consisting of 84 spectral bands in the $7.8-11.5$ μm wavelength region. The end-to-end radiometric calibration of the infrared measurements was performed using two internal calibration blackbodies. The data provided for the Contest were radiometrically and geometrically corrected. The VIS data consisted of uncalibrated, high spatial resolution, digital data with sparse ground coverage over the same area as the LWIR hyperspectral imagery [Fig. 1(b) and (e)]. The VIS data were georeferenced and registered to the thermal data.

This multisource data set presents a challenge behind the conventional multispectral and multiresolution fusion processing. It emphasizes the complementarity between spectral and thermal data in terms of information extraction. Indeed, for extracting the emissivity spectra from the LWIR data set, an extra preprocessing step is required for separating the temperature and the emissivity. Therefore, the contestants implicitly had to decide whether to use the LWIR at-sensor radiance data directly or the scene spectra and thermal variability determined through temperature-emissivity separation.

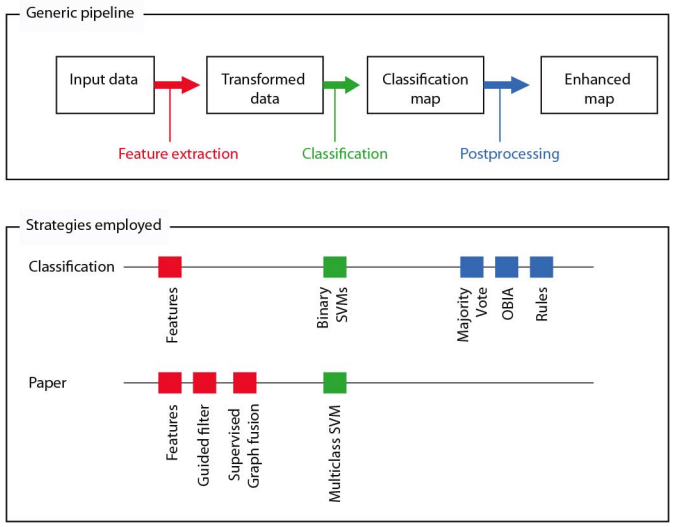

Fig. 2. Comparison of the classification approaches proposed in both tracks. Top line: the generic classification pipeline. Bottom line: the strategy proposed by each team (then detailed in Sections IV and V, respectively).

In the first stage of the Classification Contest, the participants were provided with a subset of the data [Fig. 1(a) and (b)] endowed with ground truth to train their algorithms [Fig. 1(c)]. The training map included seven classes, i.e., "road," "trees," "red roof," "gray roof," "concrete roof," "vegetation," and "bare soil." In the second stage, 1 month later, the participants received the full data set [Fig. 1(d) and (e)] and were asked to submit their classification maps with a description of the approach used within 2 weeks. The short time lap for the classification was intended to test the generalization power of the method developed on the training area with as little modification as possible. The classification was assessed using the undisclosed test samples shown in Fig. 1(f).

III. Outcomes of the 2014 Data Fusion Contest

Both winning teams of the 2014 Data Fusion Contest dealt with a classification problem. Before entering in the specific details of each method (provided in Sections IV and V, respectively), we provide a general comparison of the approaches proposed and present them with respect to a generic classification pipeline (see Fig. 2).

The generic pipeline followed by both teams included processing steps of feature extraction and classification. The winners of the Paper Contest provided most efforts in the feature extraction phase, proposing one new way of dealing with thermal features (via the guided filter) and a strategy to combine these features with morphological filters extracted from the visible data. Provided that the features extracted were meaningful, a traditional multiclass support vector machine (SVM) was used as a classifier. The winners of the Classification Contest worked mostly on the postprocessing of the classification map. They identified relevant filters and indices from the literature, and obtained a first suboptimal classification using a cascade of binary SVMs, each trained with the specific relevant features. To increase the classification accuracy, they applied a series of

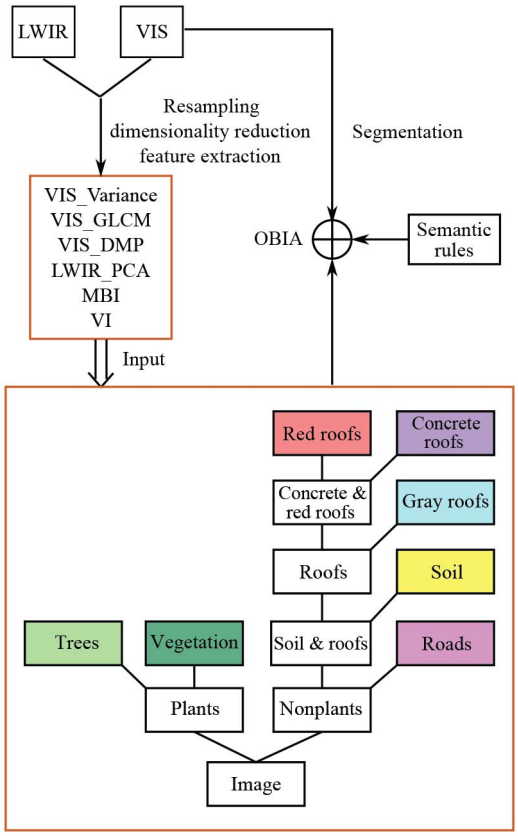

Fig. 3. Flowchart of the method proposed for the Classification Contest.

postprocessing steps: first, a majority vote on the binary pixel maps (one per class, to remove salt and pepper noise), then a multiclass filtering by majority voting within the borders of objects issued from object-based image analysis (OBIA) and finally, a correction of semantic errors using a set of predefined spatial empirical rules.

In this respect, even though both methods considered classification, the proposed approaches responded to the challenges of the two tracks of the contest: for the Classification Contest, the winners improved the initial classification map using effective production-like steps and reached maximal accuracy; while in the Paper Contest, the focus was shifted toward a new methodological contribution, with less emphasis on the geometrical precision of the final output. Of course, each approach could benefit from the other and, through this result, this contest also shows the interest of these two too often separated points of view on the classification process: on one side, the generality and discriminant nature of the data representation and, on the other, the final production stages for very precise mapping.

IV. Outcome of the Classification Contest

This section presents the hierarchical classification strategy for the fusion of LWIR and VIS data adopted by the winning team of the classification contest (Fig. 3). First, thermal infrared and VIS data were upsampled and downsampled to 0.5 m, respectively. Due to the high dimensionality of thermal infrared data, a principal component analysis (PCA) was applied and the first five principal components were kept. Then the features listed in Section IV-A were extracted. Different classes were identified successively using appropriate feature combinations (see the classification chain described in Section IV-B). Finally, the pixel-based classification map was improved by three postprocessing steps (Section IV-C): first the map was smoothed by majority voting, then it was fused with the result of an adaptive mean shift segmentation. Finally, several semantic rules were further applied to improve the result. In Sections IV-A to IV-C. detail the single blocks of the methodology, grouped by the main steps in the general pipeline highlighted in Fig. 2.

A. Feature Extraction

It is widely agreed that spatial features can significantly improve the classification accuracy due to the consideration of spatial correlation between neighboring pixels. This becomes even more relevant when considering very-high spatial resolution imagery [42], [43]. In this research, the following features were extracted.

1) *Textural features*: Occurrence and cooccurrence statistics [42], [44] were considered. For the former, features describing local variance within 3×3 and 5×5 windows were selected; for the latter, gray-level cooccurrence matrices (GLCM) were employed, using different window sizes (5, 7, and 9) and offsets of 1, 2, and 3 pixels, respectively. Then, contrast and homogeneity features were extracted. All the features above were extracted from each band of the VIS image. In addition, differential morphological profiles (DMPs) [45] were computed using the mean of the VIS image and a circular structural element (SE). The SE sizes were 2, 4, and 6, resulting in three differential opening and three differential closing profiles.
2) *Vegetation index (VI)*: 5 out of 7 classes were types of buildings or vegetation. Due to the biophysical characteristics of green plants, the normalized ratio between the average of the LWIR channels and the red band from VIS was used as VI [see Fig. 4(b)].
3) *Morphological building index (MBI)*: For buildings, the MBI [46], [47] was calculated [Fig. 4(c)]. In contrast with conventional textural or morphological features, MBI can indicate buildings directly and automatically by describing their spectral–spatial characteristics using a series of morphological operators. Specifically, the white top-hat by reconstruction is applied with a set of multidirectional linear SEs and the results are used for defining the MBI. The white top-hat is able to emphasize the bright structures with high local contrast, corresponding to the potential buildings (buildings tend to cast shadows, thus leading to large local contrast). It should be noted that MBI is calculated in an unsupervised way. The code of MBI can be found here: http://www.vhrpro.com/MBI.html.

B. Classification

In the algorithm proposed for the Classification Contest, each land cover was identified successively using a binary SVM classifier. After each classification, majority filtering was applied to suppress the salt and pepper noise of the binary map.

1) *Vegetation and trees versus the others:* Because of the significant spectral difference between green plants

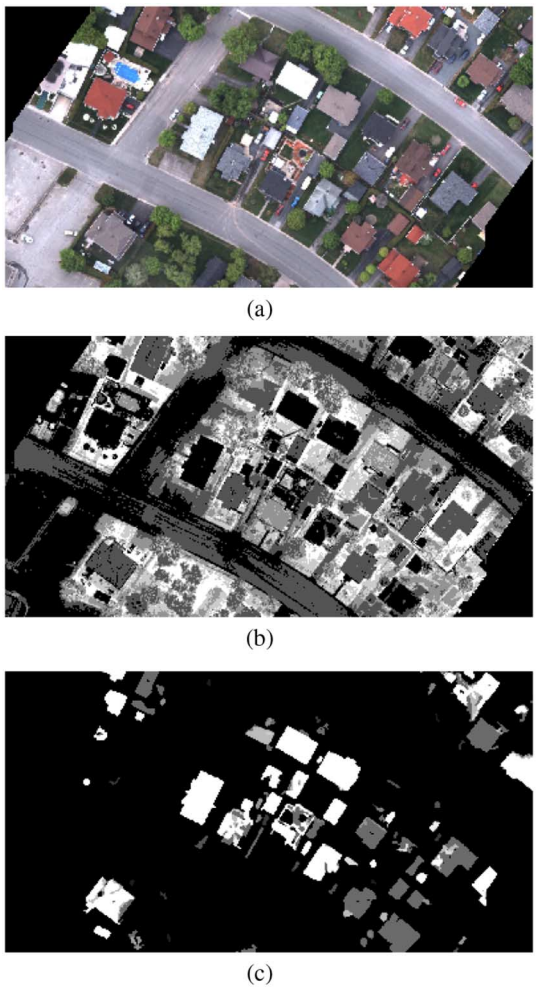

Fig. 4. Subset of (a) VIS; (b) VI; and (c) MBI.

and other classes, spectral features, including VIS and LWIR_PCA, were used in this step. After the classification, pixels classified as vegetated surfaces and with high VI (vegetation index) values were assigned to plants.

2) *Vegetation versus trees:* Although vegetation and trees share similar spectral characteristics in comparison to other classes, trees were generally lighter in the study area. They also exhibited different textural characteristics. Fig. 4(b) shows, e.g., that for trees, dark and light pixels are mixed with each other, while the vegetation class is generally smoother. The features used in the classification included the original VIS image, the textural features, and GLCM features computed on the VI (vegetation index) image, with window size of 5 and offsets of 1 and 2 pixels.
3) *Roads versus soil and roofs:* Among the classes without vegetation, roads can be easily identified due to their shape. In this step, a simple classification was first performed with VIS and LWIR_PCA and then, objects with an area smaller than 200 pixels ($50\ \mathrm{m}^2$) or showing a length–width ratio smaller than 4 were eliminated from the binary road map.
4) *Soil versus roofs:* VIS and textural features were used in this step to separate soil from roofs. The shape of roofs is more regular than that of soil areas but such information is hard to integrate into the classification. Therefore, the MBI was employed to refine the classification result by assigning all MBI objects with an area larger than 30 pixels ($7.5\ \mathrm{m}^2$) and a solidity[2] larger than 0.8 to roofs.
5) *Gray roof versus red roof versus concrete roof:* For separating the three roof types, the spectral features were preferred to textural features. In particular, gray roofs and red roofs did not show much difference in the thermal infrared imagery, whereas concrete roofs were darker than them. Therefore, gray roofs were first detected with VIS and textural features, and red roofs and concrete roofs were finally distinguished using VIS, textural, and LWIR_PCA features.

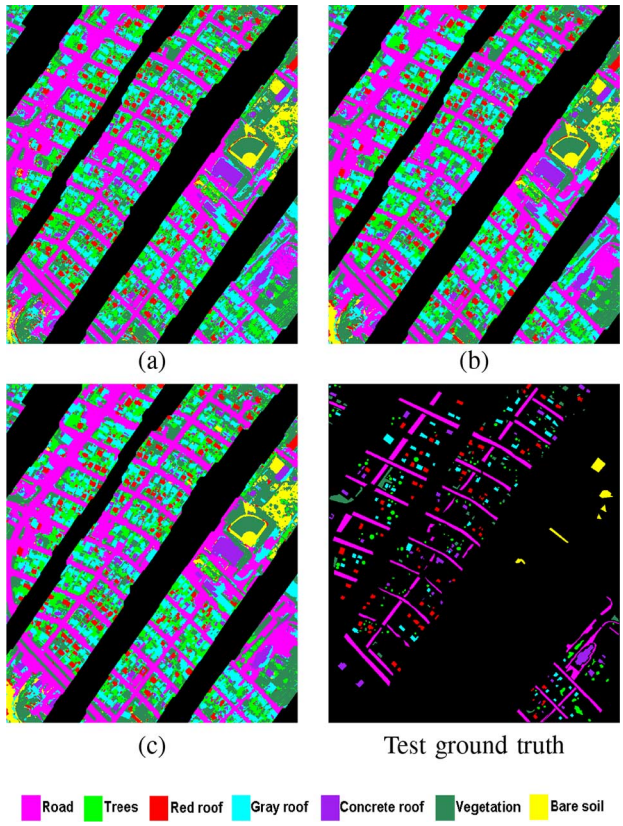

Fig. 5. Classification maps issued from the approach presented in Section IV: (a) Pixel-based; (b) object-based; and (c) final combined.

C. Postprocessing

The pixel-based classification map was then improved using three postprocessing steps.

1) *Local spatial smoothing*: As mentioned in the previous section, each binary classification map was smoothed by majority voting to enhance its spatial smoothness.
2) *Object-based image analysis*: After pixel classification, OBIA was used to refine the pixel-based classification map in Fig. 5(a). OBIA allowed to further suppress the salt and pepper effects [48] and to exploit geometrical

[2]The solidity of an object is defined as the ratio between the object area and the minimum convex area covering the object.

TABLE I
ACCURACIES OF THREE CLASSIFICATION MAPS

	OA	Kappa
Pixel-based	92.85%	0.8935
Object-based	94.69%	0.9203
Final	96.31%	0.9438

(e.g., shape) and contextual features (e.g. semantic rules for the neighboring objects) [49].

A drawback of OBIA is that the processing accuracy highly depends on the quality of the image segmentation (especially on its parameters). To reduce the uncertainty resulting from the segmentation, the adaptive mean-shift procedure [48] was used. An object-based classification map was obtained [see Fig. 5(b)] using majority voting, i.e., each object was assigned to the class to which most of the pixels composing it were assigned to in the previous processing steps.

3) *Knowledge-based refinement*: Finally, the spatial relationships between classes were investigated and the following semantic rules were applied to refine the result.
   a) If a nonroad object is totally surrounded by roads and does not belong to plants nor soil, then classify it as roads.
   b) If the area of a roof object is smaller than 20 pixels ($5\ \mathrm{m}^2$), then merge it with the neighboring object, with which it shares most of the boundary.
   c) Find all roof objects within a length–width ratio larger than 5. If such an object is adjacent to roads, then merge it with roads; otherwise, classify it as soil.

D. Results

The final result of the whole processing chain is shown in Fig. 5(c). The accuracies of the classification maps of the various steps (also shown in Fig. 5) are given in Table I. From this table, one can appreciate that both the object-based classification and the semantic rules improved the results significantly. OBIA alleviated salt and pepper effects [e.g., the soil at the bottom left corner of Fig. 5(a) and (b)], while semantic rules corrected many classification and segmentation errors [e.g., roads at the bottom right corner of Fig. 5(b) and (c)].

Such rules were not sensor- or resolution-dependent, and can, therefore, be conveniently transferred across different cities and countries with minimal adjustments of parameters.

V. OUTCOME OF THE PAPER CONTEST

This section details the methodology awarded in the Paper Contest (Fig. 6). As introduced in Section III, the proposed chain focused on the feature extraction part: first, morphological features were generated from the original VIS image (see Section V-A). In parallel, the VIS image was used in a guided filtering scheme [50] to enhance the spatial resolution of the LWIR image in the PCA domain (see Section V-B). Then, both the enhanced LWIR data and morphological VIS information were fused with a graph-based method (see Section V-C).

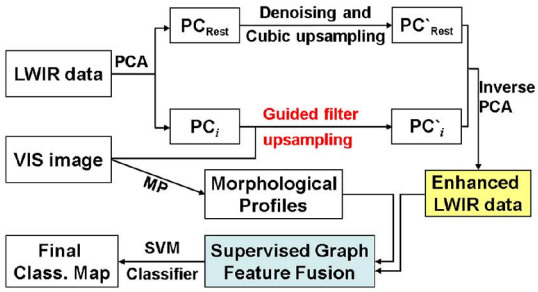

Fig. 6. Framework proposed within the Paper Contest.

Finally, the fused features were used by an SVM classifier to generate the final classification map. Since multiclass SVMs do not need particular discussion, only the three feature-extraction steps are presented in Sections V-A to V-C.

A. Morphological Features of RGB Image

Morphological features [51] were generated by applying series of morphological opening or closing by reconstruction to the image, using a structural element (SE) of predefined size. Opening acts on objects brighter than their surroundings, closing on darker objects. By increasing the size of the SE and repeating the previous operation, a complete morphological profile (MP [45]) is built. Such profile carries information about the size and the shape of objects in the image.

Morphological features are widely used to explore the spatial information of high-resolution remote sensing data [7], [52], [53]. In the method developed for the Paper Contest, morphological features were generated by applying, morphological openings and closings with partial reconstruction to the color RGB image. The effect of using morphological features with partial reconstruction for classification of remote sensing data from urban areas has been discussed in [22], [54], and [55]. MPs with ten openings and closings (ranging from 1 to 10 with step size increment of 1) were computed on the RGB image using a disk SE.

B. LWIR Data Enhancement by PCA and Guided Filter

One of the main challenges of fusing low-resolution LWIR and high-resolution VIS data is to find an appropriate balance between spectral and spatial preservation. To achieve an optimal tradeoff, a guided filtering [50] was applied to enhance the LWIR image: guided filtering performs edge-preserving smoothing on an image (in our case the LWIR), using a guidance image (in our case the VIS) that influences the result. The filtering output is locally a linear transform of the guidance image. Therefore, the structures in the guidance image will impact the filtering output. Application of the guided filter to hyperspectral data can be found in [56], where the guided filter was applied to transfer the spatial structures (e.g., edges) of the hyperspectral image to the initial classification map, in order to refine it.

To enhance the spatial resolution of the LWIR image, a PCA transform was applied along with the guided filtering presented above. Instead of using component substitutions, which may cause spectral distortions, the low-spatial resolution LWIR

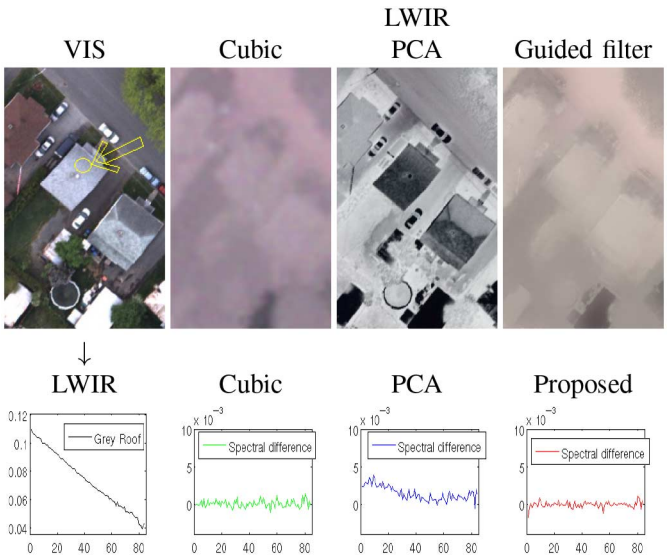

Fig. 7. Part of fused LWIR image. The top row shows VIS image and the LWIR image enhanced by cubic interpolation, PCA substitution, and the proposed guided filtering; the second row shows the original LWIR spectra from gray roof in the yellow circle and its difference with cubic interpolation, PCA substitution, and the proposed guided filtering.

image was upsampled using the high-resolution VIS image as the guidance image. To speed up processing time, first, PCA was used to decorrelate the LWIR image bands and separate information content from noise. Since they concentrate most of the energy, the guided filtering was only applied to the first k principal components (PCs) and then, the whole cube, composed of the filtered k components plus the original low-energy PCs (see Fig. 6), was inverted. Let PC_i denote the first ith ($i \leq k$) PC after upsampling with cubic interpolation. The filtering output PC_i' can be represented as a linear transform of the guidance image I_{VIS} in a local window ω of size $(2r+1) \times (2r+1)$ as follows:

$$PC_i' = a_j I_{\mathrm{VIS}} + b_j \quad \forall i \in \omega_j. \tag{1}$$

The above-mentioned model ensures that the output PC_i' has an edge only if the guided image I_{VIS} has an edge, as $\nabla PC' = a \nabla I_{\mathrm{VIS}}$. The following cost function was used to find the coefficients a_j and b_j

$$E(a_j, b_j) = \sum_{i \in \omega_j} \left[(a_j I_{\mathrm{VIS}} + b_j - PC_i)^2 + \epsilon a_j^2 \right] \tag{2}$$

where ϵ was a regularization parameter determining the degree of blurring for the guided filter. In the cost function, PC_i' should be as close as possible to PC_i, in order to ensure the preservation of the original spectral information. Before inverting, the noise from the remaining PCA channels was also removed using a soft-thresholding scheme (similarly to [57]). Their spatial resolution was also upsampled to one of the VIS images using cubic interpolation (and without guided filter). Fig. 7 shows the effectiveness of the proposed image fusion method in spectral and spatial preservation. From a visual analysis, the fused image produced by the proposed approach appears to be very sharp and spectrally consistent with respect to the original LWIR image.

C. Supervised Graph-Based Feature Fusion

Once the spectral and spatial features described in Sections V-A and V-B were extracted, they were fused using a supervised graph-based approach. This fusion strategy, which was a supervised extension of the one proposed in [22], is presented in this section. Let us define the three following quantities: $\mathbf{X}^{\mathrm{LWIR}} = \{\mathbf{x}_i^{\mathrm{LWIR}}\}_{i=1}^n$ denotes the spectral features issued from the proposed image fusion (Section V-B), $\mathbf{X}^{\mathrm{MPs}} = \{\mathbf{x}_i^{\mathrm{MPs}}\}_{i=1}^n$ are the feature vectors containing the morphological profiles computed on the VIS image (MPs, Section V-A), and $\mathbf{Y} = \{y_i\}_{i=1}^n$ are the class labels (with C possible classes). n is the number of labeled examples available. We also define the vector obtained by stacking the spectral and spatial features as $\mathbf{X}^{\mathrm{Sta}} = \{\mathbf{x}_i^{\mathrm{Sta}}\}_{i=1}^n = [\mathbf{X}^{\mathrm{LWIR}}; \mathbf{X}^{\mathrm{MPs}}]$. All data sources were scaled to the same ranges before fusion.

First, a graph was built for each data source, providing two graphs $\mathbf{G}^{\mathrm{LWIR}}$ and $\mathbf{G}^{\mathrm{MPs}}$. For example, the graph constructed using the enhanced LWIR data was $\mathbf{G}^{\mathrm{LWIR}} = (\mathbf{X}^{\mathrm{LWIR}}, \mathbf{A}^{\mathrm{LWIR}})$, $\mathbf{A}^{\mathrm{LWIR}}$ representing the edges of the graph. The edge between two data points $\mathbf{x}_i^{\mathrm{LWIR}}$ and $\mathbf{x}_j^{\mathrm{LWIR}}$ is denoted hereafter as

$$A_{ij}^{\mathrm{LWIR}} = \begin{cases} 1, & \text{if } y_i = y_j \text{ and } \mathbf{x}_j^{\mathrm{LWIR}} \in N_K^{\mathrm{LWIR}}(\mathbf{x}_i^{\mathrm{LWIR}}) \\ 0, & \text{otherwise.} \end{cases} \tag{3}$$

where $N_K^{\mathrm{LWIR}}(\mathbf{x}_i^{\mathrm{LWIR}})$ denotes the set of the K-nearest neighbors (K-NN) of $\mathbf{x}_i^{\mathrm{LWIR}}$, i.e., in the method proposed in the Paper Contest, two samples were considered close enough on the basis of a K-NN criterion. Such pairwise constraints have been recently used for aligning image pdfs in multitemporal and multisource cassification [16]. When the graph was constructed by MPs, the K-NN of the data point $\mathbf{x}_i^{\mathrm{MPs}}$ were evaluated in terms of spatial characteristics. The fusion graph was defined as $\mathbf{G}^{\mathrm{Fus}} = (\mathbf{X}^{\mathrm{Sta}}, \mathbf{A}^{\mathrm{Fus}})$, where $\mathbf{A}^{\mathrm{Fus}} = \mathbf{A}^{\mathrm{LWIR}} \bigodot \mathbf{A}^{\mathrm{MPs}}$. The operator "$\bigodot$" denotes element-wise multiplication, i.e., $A_{ij}^{\mathrm{Fus}} = A_{ij}^{\mathrm{LWIR}} A_{ij}^{\mathrm{MPs}}$

$$A_{ij}^{\mathrm{Fus}} = \begin{cases} 1, & \text{if } A_{ij}^{\mathrm{LWIR}} \bigwedge A_{ij}^{\mathrm{MPs}} = 1 \text{ and } y_i = y_j \\ 0, & \text{if } A_{ij}^{\mathrm{LWIR}} \bigvee A_{ij}^{\mathrm{MPs}} = 0 \text{ or } y_i \neq y_j. \end{cases}$$

This means that two data points $\mathbf{x}_i^{\mathrm{Sta}}$ and $\mathbf{x}_j^{\mathrm{Sta}}$ were connected only if they had similar spectral and spatial characteristics and they belonged to the same class. The fused features were extracted by projecting the high-dimensional stacked feature vector ($\mathbf{X}^{\mathrm{Sta}}$) to a lower subspace, in which neighborhood information (contained in $\mathbf{A}^{\mathrm{Fus}}$) was preserved. The projection matrix was learnt by solving a generalized eigenvalue problem similar to [58] and [59]. For more details about how to obtain the fused features, the readers can find relevant information in [22] and [59].

D. Results

The experiment considered an SVM classifier with a radial basis function (RBF) kernel. The two SVM parameters C and γ using fivefold cross-validation to find the best C within the

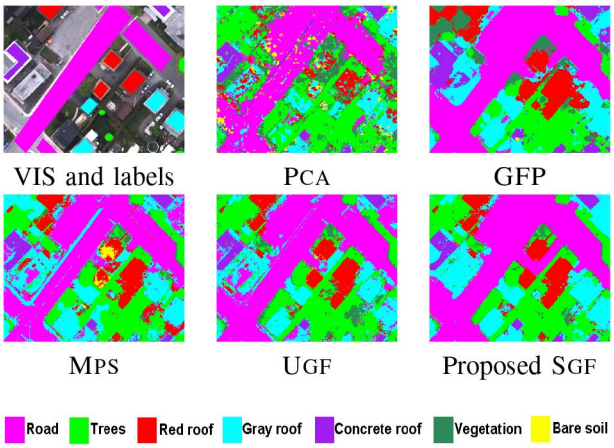

Fig. 8. Zoom in the classification maps obtained by each method.

TABLE II
CLASSIFICATION ACCURACIES AND COMPUTATION TIME (IN HOURS)

	CUB	PCA	GFP	MPS	STA	UGF	SGF
Feat.	84	84	84	60	144	23	18
OA (%)	52.6	59.9	79.0	77.5	82.4	89.9	**91.1**
AA (%)	35.1	54.6	66.8	84.8	83.3	85.6	**88.0**
κ (%)	34.7	46.3	68.7	68.8	74.7	84.8	**86.7**
Time (h)	3.81	2.82	1.17	0.67	6.86	0.61	**0.53**
Road	68.6	66.1	92.0	70.4	81.8	**94.8**	94.2
Trees	5.5	46.8	58.0	90.6	83.3	86.8	**93.6**
Red roof	53.3	37.4	73.2	93.2	96.6	96.2	**97.3**
Grey roof	34.7	48.0	61.8	79.9	80.9	81.0	**89.1**
Concrete roof	34.5	**93.9**	62.5	91.5	77.9	85.7	92.1
Vegetation	33.6	38.2	50.7	**72.5**	70.3	62.5	59.4
Bare soil	15.8	51.9	69.7	**95.7**	92.7	92.2	90.6

values $\{10^{-1}, 10^{0}, 10^{1}, 10^{2}, 10^{3}\}$ and the best γ within the values $\{10^{-3}, 10^{-2}, 10^{-1}, 10^{0}, 10^{1}\}$. The proposed fusion method (SGF) was compared against the following competitors: 1) simply enlarging the original LWIR image by cubic interpolation (CUB); 2) PCA component substitution (PCA), as in [60]; 3) our proposed image fusion using guided filtering in PCA domain (GFP); 4) using MPs computed on the original VIS image (MPS); 5) stacking our enhanced LWIR image and MPs (STA); and 6) unsupervised graph-based fusion method (UGF) [22] to fuse our enhanced LWIR image and MPs. For quantitative comparisons, 1000 samples per class were randomly selected for training, and the results were averaged over five runs. The classification results were quantitatively evaluated by measuring the overall accuracy (OA), the average accuracy (AA), and the kappa coefficient (κ) on the test data. The experiments were carried out on 64-b, 3.40 GHz Intel i7-4930 K (1 core) CPU computer with 64 GB memory. The processing time included image fusion, feature fusion, and classification. Fig. 8 shows the classification maps of the best result of each method, and Table II shows their corresponding accuracies and processing times (in hours).

The SGF feature fusion method performed better than the other fusion schemes, with more than 2% improvements in κ and a significant drop in processing time. From Table II, it is evident that using a single data source is not enough for reliable classification: for example, as the spatial information of "Red roof" and "Gray roof" or "Bare soil" is similar, objects from "Red roof" are misclassified as soil when only using MPs (see Fig. 8). Image fusion by CUB could not preserve the spatial information, leading to spatial distortions in the final classification map, whereas the PCA component substitution suffered from spectral distortions. Using the guided filter, the proposed SGF image fusion performed better on both spectral and spatial preservations, and this was reflected in classification accuracies 10% higher than CUB and PCA, especially for the class "Road." Moreover, the number of extracted fused features was smaller than for the other methods, thus further decreasing the computational time.

VI. DISCUSSION

The two tracks of the 2014 edition of the DFC provided interesting contributions in terms of methodological novelty or application to urban-area mapping. Both winning teams addressed classification problems. As discussed in more detail in Section VI-B, the fact that the winning manuscript of the Paper Contest focused on a classification problem was not surprising because of the primary role that classification plays within the IADF TC community. However, it is worth noting that significantly different approaches were adopted by the two winning teams (see also the comparison provided in Fig. 2). This is consistent with the distinct goals of the two tracks. One was aimed at optimizing the accuracy of land cover mapping for a specific data set. For this purpose, image modeling, processing, and analysis tools were adapted and integrated in a processing chain aiming at production of the most accurate map as possible. The other competition was targeted at the development of new tools for jointly taking benefit from thermal hyperspectral and color data, and a novel multisensor–multiresolution fusion method was proposed. In this Section we will comment on both these approaches and on the overall submissions to the two tracks.

A. Classification Contest results

1) Winners: With regard to the Classification Contest, the winning map was obtained through a successful integration of processing components drawn from the fields of image processing, computer vision, machine learning, and pattern recognition (see Section IV). The success of this strategy is consistent with the extremely high spatial resolution (20 cm) of the input color data and with the characteristics of the observed low-density urban area. Indeed, objects and geometrical structures were clearly apparent in the imaged scene. The definition of a) a binary decision tree adapted to the set of classes, in which case-specific feature subsets were selected for each binary node on the basis of the spectral and spatial properties of the pair of classes to be discriminated, and b) the application of rule-based criteria, in which *ad hoc* shape parameters and thresholds were used on the basis of segmentation results, were effective in characterizing the geometrical structure in the input imagery. These approaches [especially b)] are less common in the classification of coarser resolution remote

sensing data, for which spectral features usually play a primary role. Nonetheless, such approaches are well known in classical computer vision scenarios [61], [62]. Within the elaborated processing chain adopted for the Classification Contest, spatial information was exploited through both spatial-contextual feature extraction and OBIA, and the accuracy obtained using object-based classification was not significantly higher than the one that was obtained using pixel-based classification with spatial-contextual features. It is also worth noting that the winning approach for the Classification Contest could be adapted and replicated with regard to other multiresolution image classification problems involving submetric imagery, i.e., it was not tailored to the specific physical nature of the input VIS color and LWIR data. An example of these physically based approaches would involve the need to apply complex procedures to extract vegetation and trees from the scene, instead of applying a simple spectral-based rule to extract the vegetation (i.e., emissivity of vegetation is $\simeq 1$) and then, to use thermal diversity to separate the trees.

2) Top 10: Considering the other submissions received to the Classification Contest, the top-10 results[3] exhibited κ values ranging from 0.8669 to 0.9438 on the test samples. A number of image analysis and learning approaches were explored by the participants, including multiscale segmentation and region-based analysis, texture and wavelet feature extraction, feature transformations, noise filtering, Markov and conditional random fields, rule-based processing, and kernel-based and random forest classifiers. As mentioned above for the winning map, most processing approaches proposed were based on general-purpose pattern recognition concepts and were not explicitly tailored to the physical properties of color or thermal imagery.

3) Complementarity: As a last point, it is worth noting that, if a decision fusion rule is applied to these submitted results—a simple pixelwise majority—a further improvement ($\kappa = 0.9453$) is obtained. It is a minor improvement due to the already high classification accuracy of the winning map. However, it points out that the top-10 results are partly complementary, which is consistent with the different methodological approaches adopted by the various participating teams to address the classification problem proposed to the IADF community.

B. Paper Contest Results

1) Winners: The winning manuscript also addressed a classification problem (see Section V). The graph-based stages of the proposed method also were at the basis of the winning manuscript of the Best Paper Competition of the 2013 edition of DFC [22]. The successful results obtained, here with color and thermal hyperspectral data and there with LiDAR and with visible and near-infrared hyperspectral imagery, suggest the effectiveness of this graph-theoretic approach in jointly modeling multisensor remote sensing images for classification. Guided filtering, which was recently proposed and validated for image enhancement purposes, was extended here to multiresolution enhancement and found effective in the fusion of VIS and LWIR imagery. It is worth noting that this novel combination of guided filtering and graph-theoretic fusion was again not data-specific and could be extended to multiresolution and multisensor fusion problems with other input remote sensing data modalities.

2) Complementarity: Diverse methodological approaches were proposed by the participants to the Paper Contest. Besides the winning team's work presented in Section V, techniques involving decision-level fusion, morphological feature extraction, region-based processing, or rotation-forest classifiers were proposed by the top-3 ranking manuscripts.[4] Similar to the winning paper, most manuscripts submitted to the Paper Contest, including the top-3, were focused on classification problems, even though the topic of the paper was free for the participants. This came as little surprise because classification problems are the most consolidated in the DFC tradition, and represent one of the major research lines for many scientific teams that are active in the IADF community of the GRSS. However, these results also suggest that, in order to continuously offer innovative and stimulating opportunities through the annual DFC initiative, it can be important also to explore new Contest modalities and propose processing challenges that have not been considered before.

VII. Conclusion

This paper presented the scientific outcomes resulting from the 2014 Data Fusion Contest organized by the IADF TC of the IEEE GRSS. In this edition, the Contest proposed a joint multisensor–multiresolution fusion opportunity to the IADF community. A data set composed of color and thermal hyperspectral images collected over the same low-density urban area at different spatial resolutions was released. In particular, thermal hyperspectral data, which were not involved in previous Contest editions, were considered to propose an emerging type of remote sensing data to the community and stimulate the development of novel ideas and methods for their processing. The Contest was framed as two separate competitions: 1) the Classification Contest, awarding the most accurate classification result at the finest of the observed spatial resolutions, and 2) the Paper Contest, awarding methodological novelty in open-topic manuscripts using the released data.

The winning classification map was obtained through an effective case-specific processing chain that combined spectral and spatial feature extraction, binary tree decomposition, as well as object-based and knowledge-based analysis. The winning manuscript proposed a novel multiresolution and multisensor classification method that extended the recently proposed guided filtering approach to multiresolution enhancement, combined with a graph-theoretic multisensor fusion technique. The former ranked first among the classification maps obtained through diverse machine learning and pattern recognition approaches, a successful result that is likely due to an accurate

[3][Online]. Available: http://cucciolo.dibe.unige.it/IPRS/IEEE_GRSS_IADFTC_2014_Classification_Contest_Results.htm

[4][Online]. Available: http://cucciolo.dibe.unige.it/IPRS/IEEE_GRSS_IADFTC_2014_Classification_Paper_Results.htm

characterization of the target classes through suitable features, decision nodes, and rules. The latter demonstrated higher classification performances than several benchmark approaches based on previous multiresolution and/or multisensor fusion approaches, and extended the graph-theoretic approaches to supervised image fusion.

Unlike in previous editions, the Classification Contest aimed at taking into account not only the accuracy but also the computational burden. For this purpose, after the release of the full data set, a limited time was given to submit classification maps. The response of the IADF community to this competition modality was positive and very encouraging, as the number of submitted classification maps was similar to the latest Contest editions, in which there was no challenging time constraint on the submission of the final map. This confirms the choice to also implicitly consider the time taken to generate a classification result in the evaluation of the result itself, and represents a useful case study for the forthcoming Contest editions. From this perspective, a further issue that could be worth addressing is to explore other competition modalities to compare classification approaches in terms of not only accuracy but also computational properties or level of automation.

A common trait of most submissions to both tracks of the Contest was the use and/or development of processing approaches that were rooted in pattern recognition, machine learning, and image processing, and aimed at addressing the problem of joint multiresolution and multisensor fusion in its generality, while they were not specifically tailored to the physical nature of the input thermal hyperspectral and color data. On one hand, the community showed that the adopted non-physically based approaches could efficiently process the data and resolve the classification problem in an accurate way. It is also confirmed that data fusion techniques developed within remote sensing are often formulated as general methodologies that tackle broad image analysis problems and may be applied, to some extent, to multiple types of input data, sensors, and acquisition modalities.

On the other hand, incorporating prior knowledge about the physics of the data in the models, such as through temperature-emissivity separation from thermal hyperspectral samples, is expected to further improve performance (a general statement that was also confirmed in previous editions of the Contest [21]). But unfortunately, no team explored these hybrid solutions, so no answer can be given to these questions by the 2014 Contest so far. To this aim, the data released for DFC 2014 will remain publicly available in the future for further experimental analysis and for also exploring the synergy between physically based and learning/recognition-based approaches. These comments also suggest to further stimulate, through future Contests, the development of processing methods that benefit from this synergy and from explicitly modeling the physical properties of the input multisource data and of the related active and passive sensors.

ACKNOWLEDGMENT

The authors would like to thank Telops Inc. (Québec, Canada) for acquiring and providing the data used in this study, the Centre de Recherche Public Gabriel Lippmann (CRPGL, Luxembourg) and Dr. M. Schlerf (CRPGL) for their contribution of the Hyper-Cam LWIR sensor, and Dr. M. D. Martino (University of Genoa, Italy) for her contribution to data preparation. They would also thank the Award Committee for the evaluation of the submissions to the Paper Contest.

REFERENCES

[1] W. B. Gail, "Remote sensing's scale gap," *Imaging Notes*, vol. 25, no. 3, 2010.
[2] J. Zhang, "Multi-source remote sensing data fusion: Status and trends," *Int. J. Image Data Fusion*, vol. 1, no. 1, pp. 5–24, 2010.
[3] R. G. Baraniuk, "More is less: Signal processing and the data deluge," *Science*, vol. 331, no. 6018, pp. 717–719, 2011.
[4] L. Wald, "Some terms of reference in data fusion," *IEEE Trans. Geosci. Remote Sens.*, vol. 37, no. 3, pp. 1190–1193, May 1999.
[5] C. Thomas, T. Ranchin, L. Wald, and J. Chanussot, "Synthesis of multispectral images to high spatial resolution: A critical review of fusion methods based on remote sensing physics," *IEEE Trans. Geosci. Remote Sens.*, vol. 46, no. 5, pp. 1301–1312, May 2008.
[6] A. Plaza *et al.*, "Recent advances in techniques for hyperspectral image processing," *Remote Sens. Environ.*, vol. 113, (Suppl. 1), pp. S110–S122, 2009.
[7] M. Fauvel, Y. Tarabalka, J. A. Benediktsson, J. Chanussot, and J. C. Tilton, "Advances in spectral-spatial classification of hyperspectral images," *Proc. IEEE*, vol. 101, no. 3, pp. 652–675, Mar. 2013.
[8] G. Camps-Valls, D. Tuia, L. Bruzzone, and J. A. Benediktsson, "Advances in hyperspectral image classification," *IEEE Signal Proc. Mag.*, vol. 31, no. 1, pp. 45–54, Jan. 2014.
[9] L. Bruzzone and F. Bovolo, "A novel framework for the design of change-detection systems for very-high-resolution remote sensing images," *Proc. IEEE*, vol. 101, no. 3, pp. 609–630, Mar. 2013.
[10] D. Espinoza-Molina and M. Datcu, "Earth-observation image retrieval based on content, semantics, and metadata," *IEEE Trans. Geosci. Remote Sens.*, vol. 51, no. 11, pp. 5145–5159, Nov. 2013.
[11] P. Blanchart, M. Ferecatu, S. Cui, and M. Datcu, "Pattern retrieval in large image databases using multiscale coarse-to-fine cascaded active learning," *IEEE J. Sel. Topics Appl. Earth Observ. Remote Sens.*, vol. 7, no. 4, pp. 1127–1141, Apr. 2014.
[12] C. Wemmert, A. Puissant, G. Forestier, and P. Gancarski, "Multiresolution remote sensing image clustering," *IEEE Geosci. Remote Sens. Lett.*, vol. 6, no. 3, pp. 533–537, Jul. 2009.
[13] A. Voisin, V. A. Krylov, G. Moser, S. B. Serpico, and J. Zerubia, "Supervised classification of multisensor and multiresolution remote sensing images with a hierarchical copula-based approach," *IEEE Trans. Geosci. Remote Sens.*, vol. 52, no. 6, pp. 3346–3358, Jun. 2014.
[14] L. Bruzzone and M. Marconcini, "Toward the automatic updating of land-cover maps by a domain-adaptation SVM classifier and a circular validation strategy," *IEEE Trans. Geosci. Remote Sens.*, vol. 47, no. 4, pp. 1108–1122, Apr. 2009.
[15] C. Persello and L. Bruzzone, "Active learning for domain adaptation in the supervised classification of remote sensing images," *IEEE Trans. Geosci. Remote Sens.*, vol. 50, no. 11, pp. 4468–4483, Nov. 2012.
[16] D. Tuia, M. Volpi, M. Trolliet, and G. Camps-Valls, "Semisupervised manifold alignment of multimodal remote sensing images," *IEEE Trans. Geosci. Remote Sens.*, vol. 52, no. 12, pp. 7708–7720, Dec. 2014.
[17] D. Tuia, M. Volpi, L. Copa, M. Kanevski, and J. Muñoz-Marí, "A survey of active learning algorithms for supervised remote sensing image classification," *IEEE J. Sel. Topics Signal Process.*, vol. 5, no. 3, pp. 606–617, Jun. 2011.
[18] M. M. Crawford, D. Tuia, and L. H. Hyang, "Active learning: Any value for classification of remotely sensed data?" *Proc. IEEE*, vol. 101, no. 3, pp. 593–608, Mar. 2013.
[19] G. Moser, S. B. Serpico, and J. A. Benediktsson, "Land-cover mapping by Markov modeling of spatial-contextual information," *Proc. IEEE*, vol. 101, no. 3, pp. 631–651, Mar. 2013.
[20] F. Pacifici, F. Del Frate, W. J. Emery, P. Gamba, and J. Chanussot, "Urban mapping using coarse SAR and optical data: Outcome of the 2007 GRS-S data fusion contest," *IEEE Geosci. Remote Sens. Lett.*, vol. 5, no. 3, pp. 331–335, Jul. 2008.
[21] N. Longbotham *et al.*, "Multi-modal change detection, application to the detection of flooded areas: Outcome of the 2009-2010 data fusion contest," *IEEE J. Sel. Topics Appl. Earth Observ. Remote Sens.*, vol. 5, no. 1, pp. 331–342, Feb. 2012.

[22] C. Debes *et al.*, "Hyperspectral and LiDAR data fusion: Outcome of the 2013 GRSS data fusion contest," *IEEE J. Sel. Topics Appl. Earth Observ. Remote Sens.*, vol. 7, no. 6, pp. 2405–2418, Jun. 2014.
[23] G. Licciardi *et al.*, "Decision fusion for the classification of hyperspectral data: Outcome of the 2008 GRS-S data fusion contest," *IEEE Trans. Geosci. Remote Sens.*, vol. 47, no. 11, pp. 3857–3865, Nov. 2009.
[24] F. Pacifici and Q. Du, "Foreword to the special issue on optical multi-angular data exploitation and outcome of the 2011 GRSS data fusion contest," *IEEE J. Sel. Topics Appl. Earth Observ. Remote Sens.*, vol. 5, no. 1, pp. 3–7, Feb. 2012.
[25] C. Berger *et al.*, "Multi-modal and multi-temporal data fusion: Outcome of the 2012 GRSS data fusion contest," *IEEE J. Sel. Topics Appl. Earth Observ. Remote Sens.*, vol. 6, no. 3, pp. 1324–1340, Jun. 2013.
[26] G. R. Hunt, "Spectral signature of particulate minerals in visible and near infrared," *Geophysics*, vol. 42, pp. 501–513, 1977.
[27] B. D. Saksena, "Infra-red obsorption studies of some silicate structures," *Trans. Faraday Soc.*, vol. 57, pp. 242–255, 1961.
[28] O. Sandus, "A review of emission polarization," *Appl Opt.*, vol. 4, no. 12, pp. 1634–1642, 1965.
[29] C. D. B and S. Taylor, "Polarization feasibility study: Final report," Nichols Res., Tech. Rep. N-TR-97160, 1997.
[30] D. C. Bertilone, "Stokes parameters and partial polarization of far-field radiation emitted by hot bodies," *J. Opt. Soc. Amer. A*, vol. 11, no. 8, pp. 2298–2304, 1994.
[31] K. Segl, U. Heiden, S. Roessner, and H. Kaufmann, "Fusion of spectral and shape features for identification of urban surface cover types using reflective and thermal hyperspectral data," *ISPRS J. Photogramm. Eng. Remote Sens.*, vol. 58, pp. 99–112, 2003.
[32] M. Shimoni and C. Perneel, "Dedicated classification method for thermal hyperspectral imaging," in *Proc. IEEE Int. Conf. Geosci. Remote Sens. (IGARSS)*, Munich, Germany, 2012, pp. 1397–1400.
[33] G. Fontanilles, X. Briottet, S. Fabre, S. Lefebvre, and P.-F. Vandenhaute, "Aggregation process of optical properties and temperature over heterogeneous surfaces in infrared domain," *App. Opt.*, vol. 49, no. 24, pp. 4655–4669, 2010.
[34] M. Cubero-Castan, J. Chanussot, V. Achard, X. Briottet, and M. Shimoni, "A physics-based unmixing method to estimate subpixel temperatures on mixed pixels," *IEEE Trans. Geosci. Remote Sens.*, vol. 53, no. 4, pp. 1894–1906, Apr. 2015.
[35] E. Pardo-Ig, M. Chica-Olmo, and P. M. Atkinson, "Downscaling cokriging for image sharpening," *Remote Sens. Environ.*, vol. 102, no. 1–2, pp. 86–98, 2006.
[36] D. Fasbender, D. Tuia, M. Kanevski, and P. Bogaert, "Support-based implementation of Bayesian Data Fusion for spatial enhancement: Applications to ASTER thermal images," *IEEE Geosci. Remote Sens. Lett.*, vol. 5, no. 4, pp. 589–602, Oct. 2008.
[37] B. Huang, J. Wang, H. Song, D. Fu, and K. Wong, "Generating high spatiotemporal resolution land surface temperature for urban heat island monitoring," *IEEE Geosci. Remote Sens. Lett.*, vol. 10, no. 5, pp. 1011–1015, Sep. 2013.
[38] S. Delalieux *et al.*, "Unmixing-based fusion of hyperspatial and hyperspectral airborne imagery for early detection of vegetation stress," *IEEE J. Sel. Topics Appl. Earth Observ. Remote Sens.*, vol. 7, no. 6, pp. 2571–2582, Jun. 2014.
[39] J. Berni, P. J. Zarco-Tejada, L. Suarez, and E. Fereres, "Thermal and narrowband multispectral remote sensing for vegetation monitoring from an unmanned aerial vehicle," *IEEE Trans. Geosci. Remote Sens.*, vol. 47, no. 3, pp. 722–738, Mar. 2009.
[40] W. J. Emery, W. S. Good, W. Tandy, M. A. Izaguirre, and P. J. Minnett, "A microbolometer airborne calibrated infrared radiometer: The ball experimental sea surface temperature (BESST) radiometer," *IEEE Trans. Geosci. Remote Sens.*, vol. 52, no. 12, pp. 7775–7781, Dec. 2014.
[41] J. P. Allard *et al.*, "Airborne measurements in the longwave infrared using an imaging hyperspectral sensor," in *Proc. SPIE Chemical, Biological, Radiological, Nuclear, and Explosives (CBRNE) Sensing IX*, vol. 69540M, Apr. 2008.
[42] X. Huang, L. Zhang, and P. Li, "Classification and extraction of spatial features in urban areas using high-resolution multispectral imagery," *IEEE Geosci. Remote Sens. Lett.*, vol. 4, no. 2, pp. 260–264, Apr. 2007.
[43] D. Tuia, F. Pacifici, M. Kanevski, and W. J. Emery, "Classification of very high spatial resolution imagery using mathematical morphology and support vector machines," *IEEE Trans. Geosci. Remote Sens.*, vol. 47, no. 11, pp. 3866–3879, Nov. 2009.
[44] D. Marceau, P. Howarth, J. Dubois, and D. Gratton, "Evaluation of the grey-level co-occurrence matrix method for land-cover classification using Spot imagery," *IEEE Trans. Geosci. Remote Sens.*, vol. 28, no. 4, pp. 513–519, Jul. 1990.
[45] J. A. Benediktsson, J. Palmason, and J. R. Sveinsson, "Classification of hyperspectral data from urban areas based on extended morphological profiles," *IEEE Trans. Geosci. Remote Sens.*, vol. 43, no. 3, pp. 480–491, Mar. 2005.
[46] X. Huang and L. Zhang, "A multidirectional and multiscale morphological index for automatic building extraction from multispectral GeoEye-1 imagery," *Photogramm. Eng. Remote Sens.*, vol. 77, no. 7, pp. 721–732, 2011.
[47] X. Huang and L. Zhang, "Morphological building/shadow index for building extraction from high-resolution imagery over urban areas," *IEEE J. Sel. Topics Appl. Earth Observ. Remote Sens.*, vol. 5, no. 1, pp. 161–172, Feb. 2012.
[48] X. Huang and L. Zhang, "An adaptive mean-shift analysis approach for object extraction and classification from urban hyperspectral imagery," *IEEE Trans. Geosci. Remote Sens.*, vol. 46, no. 12, pp. 4173–4185, Dec. 2008.
[49] X. Huang and L. Zhang, "An SVM ensemble approach combining spectral, structural, and semantic features for the classification of high-resolution remotely sensed imagery," *IEEE Trans. Geosci. Remote Sens.*, vol. 51, no. 1, pp. 257–272, Jan. 2013.
[50] K. He, J. Sun, and X. Tang, "Guided image filtering," *IEEE Trans. Pattern Anal. Mach. Intell.*, vol. 35, no. 6, pp. 1397–1409, Jun. 2013.
[51] P. Soille and M. Pesaresi, "Advances in mathematical morphology applied to geoscience and remote sensing," *IEEE Trans. Geosci. Remote Sens.*, vol. 40, no. 9, pp. 2042–2055, Sep. 2002.
[52] A. Plaza, P. Martinez, J. Plaza, and R. Perez, "Dimensionality reduction and classification of hyperspectral image data using sequences of extended morphological transformations," *IEEE Trans. Geosci. Remote Sens.*, vol. 43, no. 3, pp. 466–479, Mar. 2005.
[53] D. Tuia, F. Ratle, A. Pozdnoukhov, and G. Camps-Valls, "Multi-source composite kernels for urban image classification," *IEEE Geosci. Remote Sens. Lett.*, vol. 7, no. 1, pp. 88–92, Jan. 2010.
[54] R. Bellens *et al.*, "Improved classification of VHR images of urban areas using directional morphological profiles," *IEEE Trans. Geosci. Remote Sens.*, vol. 46, no. 10, pp. 2803–2812, Oct. 2008.
[55] W. Liao, R. Bellens, A. Pizurica, W. Philips, and Y. Pi, "Classification of hyperspectral data over urban areas using directional morphological profiles and semi-supervised feature extraction," *IEEE J. Sel. Topics Appl. Earth Observ. Remote Sens.*, vol. 5, no. 4, pp. 1177–1190, Aug. 2012.
[56] X. Kang, J. Li, and J. A. Benediktsson, "Spectral-spatial hyperspectral image classification with edge-preserving filtering," *IEEE Trans. Geosci. Remote Sens.*, vol. 52, no. 5, pp. 2666–2677, May 2014.
[57] W. Liao *et al.*, "Hyperspectral image deblurring with PCA and total variation," in *Proc. Workshop Hyperspectral Image Signal Process. Evol. Remote Sens. (WHISPERS'13)*, Florida, USA, Jun. 2013, pp. 1–4.
[58] C. Debes *et al.*, "Hyperspectral and LiDAR data fusion: Outcome of the 2013 GRSS data fusion contest," *IEEE J. Sel. Topics Appl. Earth Observ. Remote Sens.*, vol. 7, no. 6, pp. 2405–2418, Jun. 2014.
[59] W. Liao, R. Bellens, A. Pizurica, S. Gautama, and W. Philips, "Combining feature fusion and decision fusion for classification of hyperspectral and LiDAR data," in *Proc. IEEE Int. Geosci. Remote Sens. Symp. (IGARSS'14)*, Quebec City, Canada, Jul. 2014, pp. 1241–1244.
[60] V. Shah, N. Younan, and R. King, "An efficient pan-sharpening method via a combined adaptive PCA approach and contourlets," *IEEE Trans. Geosci. Remote Sens.*, vol. 46, no. 5, pp. 1323–1335, May 2008.
[61] D. H. Ballard and C. M. Brown, *Computer Vision*. Englewood Cliffs, NJ, USA: Prentice-Hall, 1982.
[62] R. Szeliski, *Computer Vision*. New York, NY, USA: Springer, 2011.

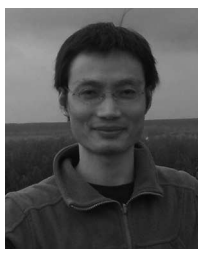

Wenzhi Liao (S'10–M'14) received the B.S. degree in mathematics from Hainan Normal University, HaiKou, China, in 2006, the Ph.D. degree in engineering from South China University of Technology, Guangzhou, China, in 2012, and the Ph.D. degree in computer science engineering from Ghent University, Ghent, Belgium, in 2012.

Since 2012, he has been working as a Postdoc with Ghent University. His research interests include pattern recognition, remote sensing, and image processing, in particular, hyperspectral image restoration, mathematical morphology, data fusion, and classification.

Dr. Liao is a member of the Geoscience and Remote Sensing Society (GRSS) and the IEEE GRSS Data Fusion Technical Committee (DFTC). He was the recipient of the "Best Paper Challenge" Awards on both 2013 IEEE GRSS Data Fusion Contest and 2014 IEEE GRSS Data Fusion Contest.

Xin Huang (M'13–SM'14) received the Ph.D. degree in photogrammetry and remote sensing from the State Key Laboratory of Information Engineering in Surveying, Mapping, and Remote Sensing (LIESMARS), Wuhan University, Wuhan, China, in 2009.

He has been working as a full Professor with LIESMARS, Wuhan University, since 2012. His research interests include hyperspectral data analysis, high-resolution image processing, pattern recognition, and remote sensing applications. He has authored more than 50 peer-reviewed articles in international journals.

Dr. Huang has been serving as an Associate Editor of the IEEE GEOSCIENCE AND REMOTE SENSING LETTERS since 2014. He was the recipient of the Top-Ten Academic Star of Wuhan University in 2009, the Boeing Award for the best paper in image analysis and interpretation from the American Society for Photogrammetry and Remote Sensing, in 2010, the New Century Excellent Talents in University from the Ministry of Education of China, in 2011. In 2011, he was recognized by the IEEE Geoscience and Remote Sensing Society as the Best Reviewer of IEEE GEOSCIENCE AND REMOTE SENSING LETTERS. In 2012, he was the recipient of the National Excellent Doctoral Dissertation Award of China. He was the winner of the IEEE GRSS 2014 data fusion contest.

Frieke Van Coillie received the M.Sc. and Ph.D. degrees in bioscience engineering (Land and Forest Management) from Ghent University, Ghent, Belgium, in 1996 and 2003, respectively.

Since 2003, she has been associated with the Faculty of Bio-science Engineering (FORSIT—Laboratory of Forest Management and Spatial Information Techniques) as a Senior Research/Teaching Scientist. Since February 2015, she has been an Appointed Professor (tenure track), with a teaching assignment in remote sensing and GIS for vegetation management. Her research interests include the interface among remote sensing, forestry, and geo-informatics. She is the author of more than 40 papers.

Dr. Van Coillie is the Associate Editor of the *International Journal of Applied Earth Observation and Geoinformation* (since 2014), and a member of the organizing resp. scientific committees of the biannual conferences GEOBIA and ForestSAT.

Sidharta Gautama (M'98) received the Diploma degree in electrical engineering in 1994 and the Ph.D. degree in applied sciences in 2002, both from Ghent University, Ghent, Belgium.

He works with the Department of Telecommunication and Information Processing, Ghent University, first as a Research Assistant and Postdoc, and since 2009 as Part-time Lecturer in computer vision. Since 2007, he has been the Head of the innovation center i-KNOW, Ghent University, which incubates the licensing and spin-off activity of the research in intelligent information processing.

Aleksandra Pižurica (M'03) received the Diploma Degree in electrical engineering from the University of Novi Sad, Novi Sad, Serbia, in 1994, the Master of Science degree in telecommunications from the University of Belgrade, Belgrade, Serbia, in 1997, and the Ph.D. degree in engineering from Ghent University, Ghent, Belgium, in 2002.

From 1994 till 1997, she was working as a Research and Teaching Assistant with the Department of Telecommunications, University of Novi Sad. In 1997, she joined the Department of Telecommunications and Information Systems, Ghent University, first as a Ph.D. student and later as a Postdoctoral Research Fellow (with the fund for scientific research in Flanders-FWO Vlaanderen) and Part-time Lecturer. Since 2011, she has been a Full-time Professor with Ghent University in statistical image modeling. She has Founded Statistical Image Modeling Laboratory, Ghent University and she is also leading the Research Unit Video and Image Content Analysis (VICA) of inter-university research Department "Future Media and Imaging" of the Flemish iMinds Institute. Her research interests include statistical image modeling, multiresolution and sparse signal representations, Bayesian estimation, and applications in video analysis, remote sensing, and medical imaging.

Dr. Pižurica is currently serving as an Associate Editor for the IEEE TRANSACTIONS ON IMAGE PROCESSING.

Wilfried Philips (S'90–M'93–SM'10) was born in Aalst, Belgium, on October 19, 1966. He received the Diploma degree in electrical engineering and the Ph.D. degree in applied sciences both from Ghent University, Ghent, Belgium, in 1989 and 1993, respectively.

From October 1989 until October 1997, he worked with the Department of Electronics and Information Systems, Ghent University for the Flemish Fund for Scientific Research (FWO-Vlaanderen), first as a Research Assistant and later as a Postdoctoral Research Fellow. Since November 1997, he has been with the Department of Telecommunications and Information Processing, Ghent University, where he is currently a Full-time Professor and is the Head of the research group "Image Processing and Interpretation," which has recently become part of the virtual Flemish ICT Research Institute iMinds. His research interests include image and video restoration, analysis and the modeling of image reproduction systems, remote sensing, surveillance, and industrial inspection.

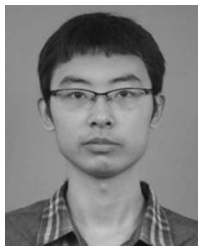

Hui Liu received the B.S. degree in mathematics from Wuhan University, Wuhan, China, in 2012, where he is currently pursuing the Ph.D. degree at the State Key Laboratory of Information Engineering in Surveying, Mapping, and Remote Sensing, Wuhan University, Wuhan, China.

His research interests include image processing, object recognition, and remote sensing applications.

Tingting Zhu received the B.S. degree from Nanjing Normal University, Nanjing, China, in 2012, and the M.S. Degree from the State Key Laboratory of Information Engineering in Surveying, Mapping, and Remote Sensing (LIESMARS), Wuhan University, Wuhan, China, in 2014. She is currently pursuing the Ph.D degree at LIESMARS.

Her research interests include change detection from high-resolution remotely sensed imagery, and the polar remote sensing.

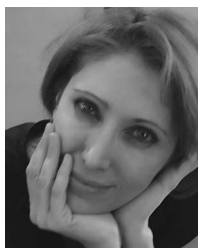

Michal Shimoni (M'08) received the M.Sc. degree from Tel Aviv University, Tel Aviv, Israel, in 1997, the Civil Engineering studies from the University of Gembloux, Belgium, in 1999, and the Ph.D. degree from TUDelft, Delft, The Netherlands, in 2004.

Since 1999, she has been employed as a Senior Researcher with the Signal and Image Centre, Belgian Royal Military Academy, Brussels, Belgium. Her research interests include imaging spectroscopy, PolSAR, PolInSAR, and multisensor fusion. In imaging spectroscopy, her researches focus on thermal hyperspectral, mixing models, target and change detection, classification based spectroscopy and spatial and spectral fusion for complex urban areas.

Gabriele Moser (S'03–M'05–SM'14) received the Laurea (M.Sc. equivalent) degree in telecommunications engineering and the Ph.D. degree in space sciences and engineering from the University of Genoa, Genoa, Italy, in 2001 and 2005, respectively.

Since 2014, he has been an Associate Professor of Telecommunications with the University of Genoa. Since 2001, he has been cooperating with the Image Processing and Pattern Recognition for Remote Sensing (IPRS) Laboratory, University of Genoa. From January to March 2004, he was a Visiting Student at the Institut National de Recherche en Informatique et en Automatique (INRIA), Sophia Antipolis, France. He is the Head of the Remote sensing for Environment and Sustainability (RIOS) Laboratory, University of Genoa. His research interests include the development of image-processing and pattern-recognition methodologies for remote-sensing data interpretation, multisource data fusion, contextual classification, change detection, kernel-based learning, and geo/biophysical parameter estimation.

Prof. Moser has been a Reviewer for several international journals. He has been an Associate Editor of the international journals IEEE GEOSCIENCE AND REMOTE SENSING LETTERS and *Pattern Recognition Letters* since 2008 and 2011, respectively. He is the Chairman of the Image Analysis and Data Fusion Technical Committee of the IEEE Geoscience and Remote Sensing Society. He is a Program Co-Chair of the EARTHVISION Workshop at the 2015 Computer Vision and Pattern Recognition Conference. He was the recipient of the Best Paper Award at the 2010 IEEE Workshop on Hyperspectral Image and Signal Processing.

Devis Tuia (S'07–M'09–SM'15) was born in Mendrisio, Switzerland, in 1980. He received the Diploma degree in geography from the University of Lausanne (UNIL), Lausanne, Switzerland, in 2004, the Master of Advanced Studies in environmental engineering from the Federal Institute of Technology of Lausanne (EPFL) in 2005, and the Ph.D. degree in environmental sciences from UNIL, in 2009.

He was a Visiting Postdoc Researcher at the University of Valéncia, Valéncia, Spain, and the University of Colorado, Boulder, CO, USA. He then worked as Senior Research Associate with ÉPFL under a Swiss National Foundation program. Since 2014, he has been an Assistant Professor with the Department of Geography, University of Zurich, Zurich, Switzerland. His research interests include the development of algorithms for information extraction and data fusion of remote sensing images using machine learning algorithms.

Dr. Tuia serves as a Co-Chair of the Image Analysis and Data Fusion Technical Committee of the IEEE GRSS. He is an Associate Editor of the IEEE JOURNAL OF SELECTED TOPICS IN APPLIED EARTH OBSERVATION AND REMOTE SENSING.